Review of design parameters for FRP-RC members detailed according to ACI 440.1R-06

Fares Jnaid and Riyad Aboutaha[*]

Department of Civil and Environmental Engineering, Syracuse University, Syracuse, NY, USA

Abstract. This paper investigates the parameters that control the design of Fiber Reinforced Polymer (FRP) reinforced concrete flexural members proportioned following the ACI 440.1R-06. It investigates the critical parameters that control the flexural design, such as the deflection limits, crack limits, flexural capacity, concrete compressive strength, beam span and cross section, and bar diameter, at various Mean-Ambient Temperatures (MAT). The results of this research suggest that the deflection and cracking requirements are the two most controlling limits for FRP reinforced concrete flexural members.

Keywords: GFRP; steel; flexural strength; deflection; cracking; reinforcement ratio

1. Introduction

In severe environments, the primary durability problem that faces steel reinforced concrete structures is the corrosion of rebars. Non-metallic rebars could be used as concrete reinforcement, e.g. Fiber Reinforced Polymer (FRP) composites.

This paper presents the impact of various parameters on the design of concrete flexural members reinforced with Glass Fiber Reinforced Polymer (GFRP) bars. Following the recommendations of the ACI 440.1R-06 guideline (2006), this study investigates the effects of the following factors on the flexural response of beams: the area of FRP reinforcement, beam span length and cross section, Mean-Ambient-Temperature [MAT], deflection limits, cracking limits and concrete compressive strength. A comparison between the design of GFRP and steel reinforced concrete members is also presented.

2. FLEXURAL DESIGN PHYLOSOPHY: (ACI 440.1R-06)

2.1 Flexural strength

Since steel yields before rupture, steel reinforced concrete structures are designed to be under-reinforced, so steel yields before crushing of concrete. On the other hand, because the FRP bars do

---

not yield, it is a necessity to reconsider this approach, and allow crushing of concrete before fracture of the FRP bars. The concrete crushing failure mode is more desirable for flexural members reinforced with FRP bars (Nanni 1993b).

Fig. 1 shows the stress, strain, and internal forces for the three possible cases of a rectangular section reinforced with FRP bars, in bending. Failure modes (FRP rupture or concrete crushing) are acceptable in governing the design of flexural members reinforced with FRP bars provided that strength and serviceability criteria are satisfied. To compensate for the lack of ductility, the member should possess a higher reserved strength. The margin of safety suggested by this guide against failure is therefore higher than that used in traditional steel-reinforced concrete design.

If the reinforcement ratio is less than the balanced ratio ($\rho_f < \rho_{fb}$), FRP rupture failure mode governs. Otherwise, concrete crushing governs. Table 1 reports some typical values for the balanced reinforcement ratio, note that the balanced ratio for FRP reinforcement ρ_{fb} is much lower than both the balanced ratio for steel reinforcement ρ_b and the minimum reinforcement ratio for steel ($\rho min = 0.0035$ for Grade 60 steel and $f_c' = 5000$ psi [35 MPa]).

(a) Failure governed by concrete crushing

(b) Balanced failure condition

(c) *Failure governed by GFRP rupture (concrete stress may be non-linear)*
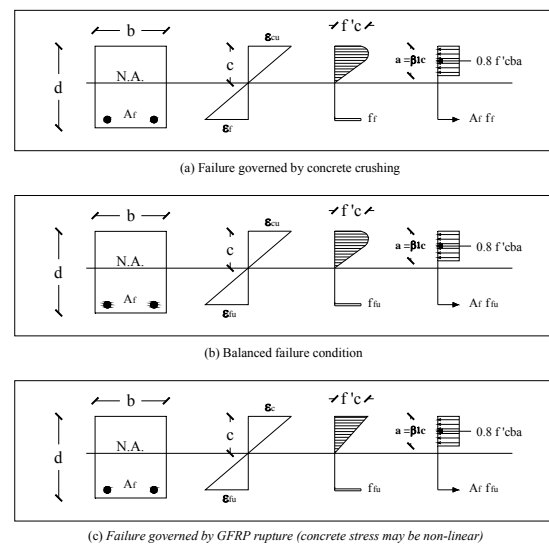
Fig. 1 Stress and strain distribution at ultimate condition (ACI 440.1R-06)

Table 1 Typical values for balanced reinforcement ratio for a rectangular section with $fc' = 5000$ psi (34.5 MPa) (ACI 440.1R-06)

Bar type	Yield strength fy or tensile strength ffu, ksi (MPa)	Modulus of elasticity, ksi (GPa)	ρ_b or ρ_{fb}
Steel	60 (414)	29,000 (200)	0.0335
GFRP	80 (552)	6000 (41.4)	0.0078
AFRP	170 (1172)	12,000 (82.7)	0.0035
CFRP	300 (2070)	22,000 (152)	0.002

Nominal flexural strength: When $\rho_f > \rho_{fb}$, crushing of the concrete controls the failure of the member, and the stress distribution in the concrete can be approximated with the ACI rectangular stress block (shown in Fig. 1).

When $\rho_f < \rho_{fb}$, rupture of FRP bars control the failure mode, and since the maximum concrete strain (0.003) may not be reached, the ACI stress block is not applicable.

Strength reduction factor for flexural: In order to insure an adequate level of safety in an FRP member, a conservative strength reduction factor must be applied. That is due to the fact that FRP members do not demonstrate ductile behavior. Fig. 2 shows the linear transition between the two failure modes mentioned above.

2.2 Serviceability

The majority of research with FRP bars for reinforcing concrete has been on simply supported beams and slabs where the low value of elasticity of FRP has meant that the service behaviors has been critical (Zheng *et al.* 2012).

Serviceability control is a major concern in (FRP) reinforced concrete members. This due to the small stiffness these members have after cracking. Therefore, it is important to consider designing cross-sections for concrete crushing.

Serviceability has been reported to control the design by many researchers such as (Bischoff *et al.* 2009, Shield *et al.* 2011, Veysey and Bischoff 2011).

"Because of the low stiffness of the FRP reinforcement in flexural concrete members reinforced with fiber reinforced polymer (FRP) bars, serviceability requirements related to deflection and crack widths often control the design", (Bischoff and Gross 2011).

The indirect deflection control design provisions by ACI 440.1R-06 are based on the following equation by Ospina *et al.* (2001). Ospina and Gross (2005), modified the same equation by the ratio I_e/I_g to account for concrete's tension stiffening in the minimum members depth predictions. This led to the recommended minimum thickness of non-prestressed beams or one-way slabs adopted by the ACI 440.1R-06.
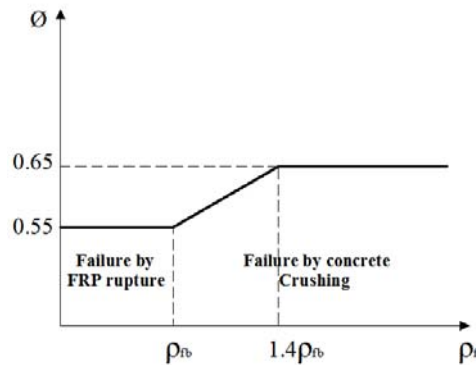

Fig. 2 Strength reduction factor as a function of the reinforcement ratio (ACI 440.1R-06)

However, the minimum member thickness requirements of ACI 440.1R-06 do not guarantee that all deflection considerations will be satisfied in a project, Ospina *et al.* (2007).

Direct deflections in ACI 440.1R-06 are calculated based on Branson's equation using the effective moment of inertia I_e, Gao *et al.* (1998a) concluded that to account for reduced tension stiffening in FRP-reinforced members, a modified expression for the effective moment of inertia is required. They suggested adding a reduction coefficient, β_d, which is related to the reduced tension stiffening exhibited by FRP-reinforced members.

Ospina *et al.* (2007) pointed out that β_d is dependent on ρ_{fb}. They suggested that this is incorrect because ρ_{fb} is related to the ultimate tensile strength f_{fu}, while the deflection calculation is a problem associated with serviceability limit state,

Bischoff (2005) suggested an alternative equation for the effective moment of inertia which does not take into account the empirically-tuned term β_d.

Moreover, Bischoff and Gross (2011), suggested calculating deflection with an equivalent moment of inertia I'_e based on integration of curvature (M/E_cI_e) to account for changes in member stiffness along the span. They evaluated the results for both steel and FRP reinforced concrete members under different support conditions and loading arrangements.

Nevertheless, Bischoff and Gross (2011) stated that "the most current expression used by ACI Committee 440 (2006) provides reasonable estimates of computed deflection for members reinforced with glass FRP (GFRP) and carbon FRP (CFRP)".

The reference crack width limits for an exterior beam is 0.5 mm. Ospina and Bakis (2006), proposed a discontinuous representation of the ACI 440.1R-06 equation to solve for the maximum bar spacing taking into account the crack width limits specified by the codes (Ospina and Nanni 2007).

3. Investigation of the critical design parameters for GFRP reinforced concrete flexural members

This paper was conducted to help engineers understand the behaviour of the GFRP reinforced concrete members (FRP-RCM) under various physical and environmental loading conditions/states. This research investigates the factors that control the design FRP-RCMs, and compares GFRP, and steel as concrete reinforcement to identify the most efficient material for different cases of loading. The recommendations of the (ACI 440.1R-06) were followed to investigate the effects of the followings: Amount of FRP reinforcement, beam span length , the aspect ratio of the beam cross section, the Mean-Ambient-Temperature [MAT], the deflection design limits, the cracking design, limits on load carrying capacity, the concrete compressive strength and a Comparison between GFRP and steel reinforcements.

The modified guaranteed ultimate tensile properties of the GFRP bars at various temperatures are provided by Schöck Bauteile GmbH, a Germany company which design GFRP rebars called ComBar®, and are listed in Table 2.

The program used to conduct the analysis was written in Visual Basic for Applications VBA, based on (ACI 440.1R-06) recommendations, the program saves the analysis results on an excel sheet platform, which helps the user transferring the data into charts.

3.1 Effect of the reinforcement ratio (ρ_f)

Table 2 Modified guaranteed ultimate tensile properties (Aboutaha 2006)

Temperature (℃)	GFRP	
	f^*_{fu} (MPa)	E_f(MPa)
20	1000	60000
40	850	58000
60	700	56000

The following different combinations were investigated, b x h = (900 x 300) mm, (900 x 450) mm, (450 x 450) mm, (450 x 900) mm and (300 x 900) mm, where b, h are width and the height of the cross-section respectively. The compressive strength of concrete was assumed to be 30 MPa. The modified guaranteed ultimate tensile properties of the GFRP bars at various temperatures are shown in Table 2.

The charts produced present the nominal flexural capacity versus the reinforcement ratio (ρ_f). Fig. 3 gives an idea about the FRP ratio (ρ_f) effect, the X axis is the reinforcement ratio, while the left Y axis is the value of nominal flexural strength (M_n) divided by bd², to exclude the effect of the beam dimensions, the right Y axis is the value of the effective stress (f_f) in the FRP bars. A close look at the figures shows that increasing the amount of the FRP reinforcement area is associated with increase in the nominal flexural strength (M_n). On the other hand, an increase in reinforcement area results in decrease in the stress level. Notice that when the reinforcement ratio is smaller than the one at the balanced condition ($\rho_f < \rho_{fb}$), the rate of increase in the flexural capacity is higher than those when ($\rho_f > \rho_{fb}$). This means that a small increase in the reinforcement ratio leads to a large increase in the flexural capacity when ($\rho_f < \rho_{fb}$). That is due to the fact that when ($\rho_f < \rho_{fb}$), the FRP rupture failure mode governs, and the bars are highly stressed, whereas when ($\rho_f > \rho_{fb}$), the concrete crushing controls. Therefore, it is less efficient to use reinforcement ratio much larger than the ratio at the balanced condition.
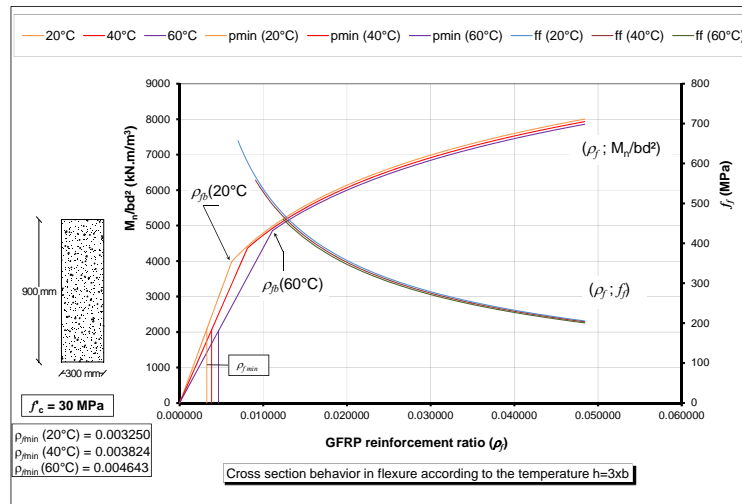
Fig. 3 M_n/bd^2 and f_f vs. ρ_f for an h/b=3 cross section

3.2 Effect of mean-ambient-temperature [MAT]

All the cases mentioned above were investigated at the following temperatures (20°, 40°, 60°) Celsius. The same amount of bars means the same amount of reinforcement ratio, because the concrete cross sections are the same. Notice that for the same reinforcement area, the higher the temperature, the lower the beam's nominal flexural strength. That is because when the temperature increases, the ultimate tensile strength of the FRP bars decreases. In addition, the offset between the curves is larger when $\rho_f > \rho_{fb}$. This means that a slight change in the amount of bars leads to a large change in the difference between the ultimate strength due to different temperatures. Furthermore, for the same amount of reinforcement, the difference between the ultimate flexural strength under various temperatures when ($\rho_f < \rho_{fb}$) is larger than when $\rho_f > \rho_{fb}$. That is because when the reinforcement amount is less than the one needed for the balanced condition, the FRP bars are highly stressed. On the other hand, when ($\rho_f > \rho_{fb}$), the bars are much less stressed. Thus, the impact of the MAT is much less when $\rho_f > \rho_{fb}$.

3.3 Effect of the span length and the other parameters that control the design

FRP reinforced concrete beams exhibit large deflections and wider cracks, as the FRP bars have low modulus of elasticity compared to steel. The design of FRP-RCMs is very likely to be controlled by these two parameters. This study investigates all the parameters that control the flexural design of FRP-RCMs; which includes the beam length, the aspect ratio of the concrete section, deflection limits, and crack width limits.

Fig. 4 shows the matrix of the beams that were investigated. A set of W_{LL}-ρ_f curves were constructed based on the nominal flexural strength, deflection limits, and crack width limits. Design curves were developed for beams reinforced with GFRP bars. In addition, two beam sections were adopted: (1) (h=1000 mm, b=500 mm) and (2) (h=500 mm, b=1000 mm). Three beam spans were also adopted for this investigation, L=5 m, L=7.5 m, L=10 m. Following the ACI 440.1R-06 recommendations, the deflection serviceability limits of L/240, L/360 and L/480 were adopted. The limit L/240 is required for roof or floor constructions supporting or attached to nonstructural elements not likely to be damaged by large deflections. While the limit L/480 is required for roof or floor constructions supporting or attached to nonstructural elements likely to be damaged by large deflections. The term L/360 is required for floors not supporting or attached to nonstructural elements likely to be damaged by large deflections. The beams investigated in this section were considered exterior and exposed to earth and weather, and therefore, the crack width limit was 0.5 mm. The concrete compressive strength used for all beams in this section was 25 MPa.

In order to calculate the maximum live-load that can be carried by the beam when the serviceability limit states controls the design, a computer program was developed and an iteration method was used to obtain those values. The software calculates the live-load that can be carried by the beam based on ultimate limit state and serviceability for 13 different reinforcement ratios and saves the outcomes to an excel file. Fig. 5 shows the algorithm used for calculating W_{LL} based on the deflection limits. Notice that the variable j in the chart varies from 1 to 13 which is the number of points on the (W_{LL}) vs. ρ_f charts that will be discussed later.

Fig. 4 The different combinations in calculating W_{LL}

Fig. 5 The algorithm used for calculating W_{LL} based on the deflection limits
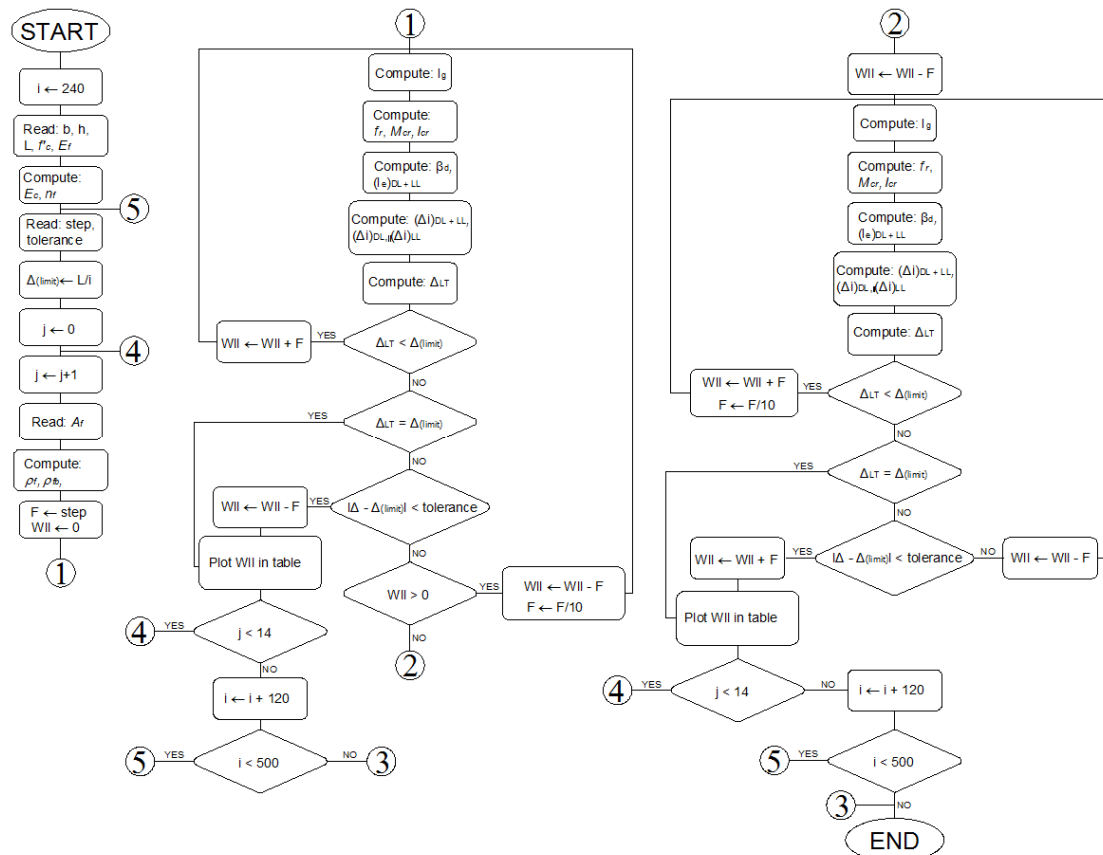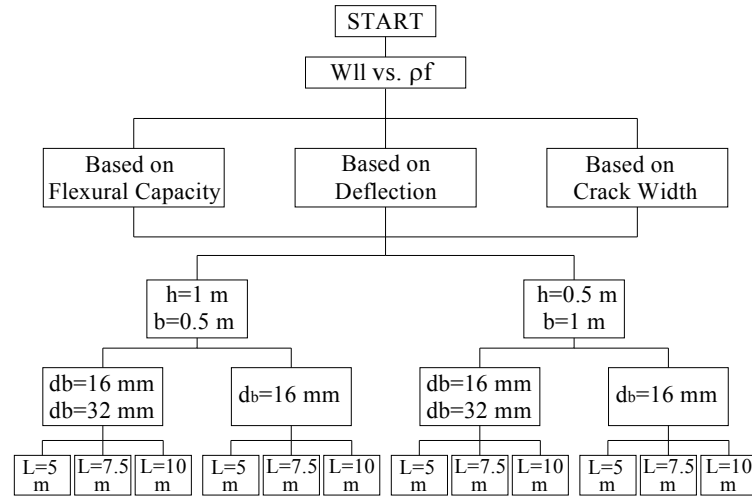
3.4 Effect of beam span and cross section

As shown in the matrix above, many combinations were investigated in order to have a clear view of the parameters that control the design. Figs. 6 and 7 show the live load (W_{LL}) vs. ρ_f for some of the many combinations mentioned above at 20°C, a 7.5 span beam with h=1000 mm and b=500 mm when using both 16 mm and 32 mm bar diameters and when using only 16 mm bar diameter.

Note that in the case of deflection, when using both 16,32 mm bar diameter, there is a slight change in the slope at the ninth point. This is because at the tenth point, two layers of reinforcement have been used, which means that d is decreasing, thus, the cracking moment of inertia is smaller, which leads to a lower value of $(I_e)_{DL + LL}$. On the other hand, since the value of M_n is directly proportional to the value of d, the change in the curve's slope after the ninth point is
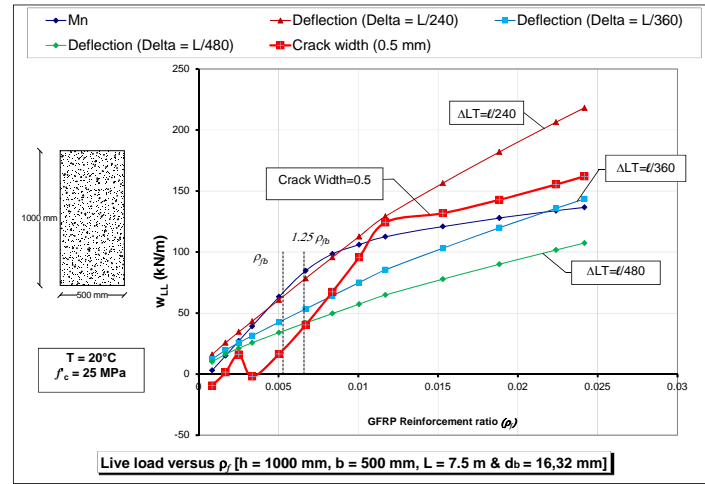

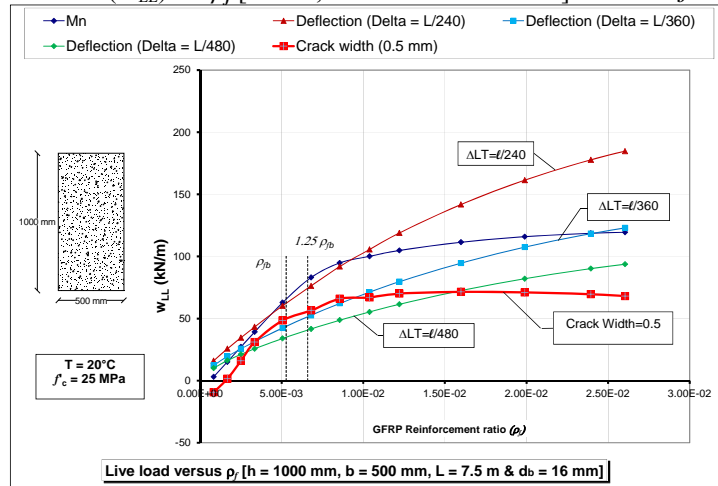Fig. 6 Live load (W_{LL}) vs. ρ_f [h=1 m, b=0.5 m and L=7.5 m] at 20°C d_b=16,32 mm

Fig. 7 Live load (W_{LL}) vs. ρ_f [h=1 m, b=0.5 m and L=7.5 m] at 20°C d_b=16 mm

larger when M_n, rather than when the deflection, is controlling the design. Moreover, when investigating Chart 6, it is obvious that there is a noticeable change in slope of the curves at the fourth point. This is because the bar diameter was changed from 16 to 32. So, instead of using 8 bars No. 16, two bars No. 32 were used, which resulted in an increase in the bar spacing s, and because the crack width is connected directly to the space between the bars, for a larger s and the same crack width limit, the W_{LL} that the beam can carry decreases. The last four points of the curves experience a decrease in slope, this happens when two layers of reinforcement are used, which results in a decrease in d value. Also, there is a change in the slope of the deflection curve at the sixth and eighth points in Fig. 7, this is due to using two and three layers of steel respectively.

Table 3 Factors that control the design ($\Delta LT=L/240$)

	$\Delta LT=L/240$			
	h=1 m b=0.5 m		h=0.5 m b=1 m	
	d_b=16, 32 mm	d_b=16 mm	d_b=16, 32 mm	d_b=16 mm
L=5 m	Crack	Crack	Crack	Crack, Deflection
L=7.5 m	Crack	Crack	Crack	Deflection
L=10 m	Crack	Deflection	Crack	Deflection

Table 4 Factors that control the design ($\Delta LT=L/360$)

	$\Delta LT=L/360$			
	h=1 m b=0.5 m		h=0.5 m b=1 m	
	d_b=16, 32 mm	d_b=16 mm	d_b=16, 32 mm	d_b=16 mm
L=5 m	Crack	Crack	Crack	Deflection
L=7.5 m	Crack	Deflection	Crack	Deflection
L=10 m	Crack	Deflection	Crack	Deflection

Table 5 Factors that control the design ($\Delta LT=L/480$)

	$\Delta LT=L/480$			
	h=1 m b=0.5 m		h=0.5 m b=1 m	
	d_b=16, 32 mm	d_b=16 mm	d_b=16, 32 mm	d_b=16 mm
L=5 m	Crack	Crack	Crack	Deflection
L=7.5 m	Crack	Deflection	Crack	Deflection
L=10 m	Crack, Deflection	Deflection	Crack	Deflection

Tables 3-5 show the parameters that control the design for all the cases studied.

Looking at Tables 3-5, it can be seen that when 32-mm bar diameter was used, and for the reinforcement ratio ($\rho_{fb} < \rho_f < 1.25\rho_{fb}$), crack width limits control 95% of the cases. The other cases are controlled by the crack width partially, meaning that when ρ_f is in the recommended reinforcement range, the crack width only controls a part of that range. For instance, when $\rho_f = \rho_{fb}$, the design is controlled by deflection and as this ratio increase it reaches a certain point in the previous range where the crack starts to control the design. However, deflection does not control any of the previous cases completely. This is because when using reinforcing bars of 32 mm diameter, the balanced condition occurs when only 3 bars are used, so the spacing between the bars is large, which leads to cracking dominated behavior. Therefore, since the effect of bar diameter on the flexural and deflection is limited, it is recommended that more small diameter bars rather than fewer large diameter bars be used.

When 16 mm diameter bars were used, with *L*, *h*, *b* equal 5, 1, 0.5 meters respectively, and when $\Delta_{LT}=L/240$ or $\Delta_{LT}=L/360$, crack width controls all the cases. Moreover, when the deflection limit is *L*/480 and the reinforcement is GFRP, crack width controls the design, which leads to the conclusion that short and deep beams tend to be controlled by crack width, furthermore, the larger the applied load that, the more likely that deflection controls the design. Moreover, for the same beam section, when *L*=7.5 m, crack width controls only when the deflection limit is *L*/240, while the deflection controls all other cases. Also, when *L*=10 m, deflection controls for all cases except for the case when $\Delta_{LT}=L/480$. This last case is controlled by both crack and deflection. All these cases support the same conclusion mentioned above.

When 16 mm GFRP reinforcing bars were used, with *h*=500 mm and *b* =1000 mm, deflection controls for all cases, except when *L*=5 m and $\Delta_{LT}=L/240$ where both the deflection and the crack width control.

Moreover, Figs. 8 and 9 show the live load (W_{LL}) vs. ρ_f for 7.5 m and 10 m span beams respectively. The height of the cross section is *h*=500 mm and the width is *b*=1000 mm, the rebars diameter is 16 mm. It can be observed that when the length of the beam is 7.5 m and within the recommended reinforcement ratio, the beam can carry a live load which is equal or smaller than its own weight based on the deflection limit. However, when the span is 10 m, and for the same reinforcement ratios, the beam is unable to carry its own self-weight. Thus, it is not recommended to use FRP as reinforcement when the span to depth ratio is larger than 15.
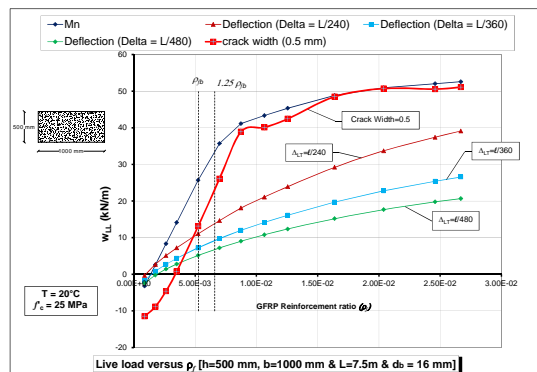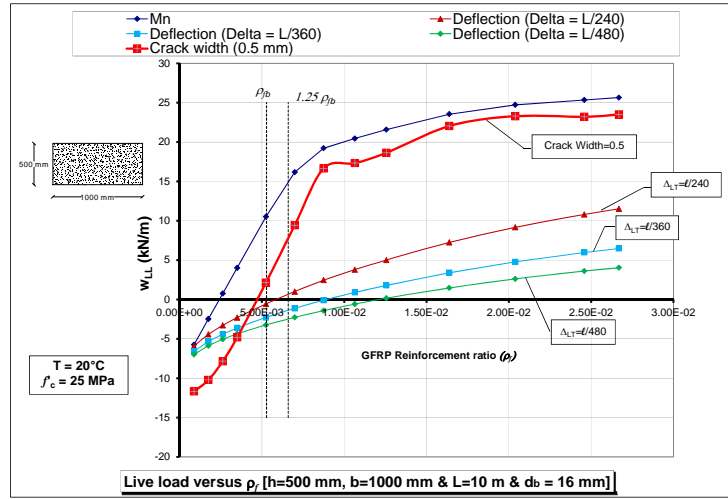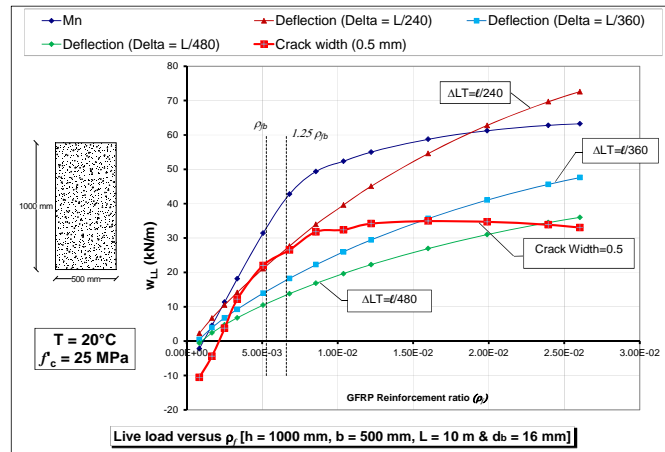

Fig. 8 Live load (W_{LL}) vs. ρ_f [*h*=0.5 m, *b*=1 m and *L*=7.5 m] at 20°C d_b=16 mm

Fig. 9 Live load (W_{LL}) vs. ρ_f [h=0.5 m, b=1 m and L=10 m] at 20°C d_b=16 mm

Fig. 10 Live load (W_{LL}) vs. ρ_f [h=1 m, b=0.5 m and L=10 m] at 20°C d_b=16 mm

3.5 Effect of temperature on the factors that control the design

Charts 10, 11, show W_{LL} vs. ρ_f under different temperatures (20°C, 60°C) for GFRP reinforced beam, using 16 mm bar diameter, with a span length of 10 m and a cross-section of h=2 x b. The charts show that the value of ρ_{fb} increases as the temperature increases. This is because when the temperature rises, the guaranteed ultimate tensile strength and modulus of elasticity decrease. In other words, for the same amount of reinforcement, high temperatures decrease the beam capacity. They also show that for a deflection limit of Δ_{LT}=L/240 and when ($\rho_{fb}<\rho_f<1.25\rho_{fb}$) and for a 60 degree C, the Crack width controls the design. This is also applicable for a 20 degree C only when ($\rho_f>1.15\rho_{fb}$). Whereas for the same deflection limit, when T = 20 degree C and ($\rho_{fb}<\rho_f<1.15\rho_{fb}$) the crack width controls the design.
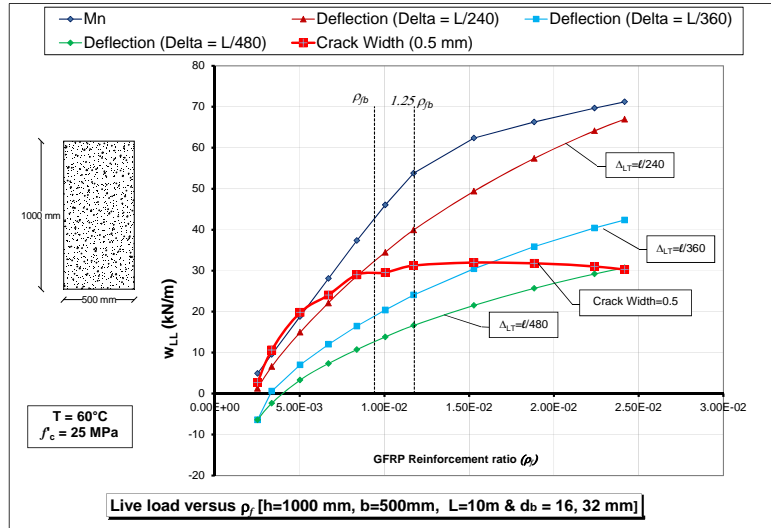
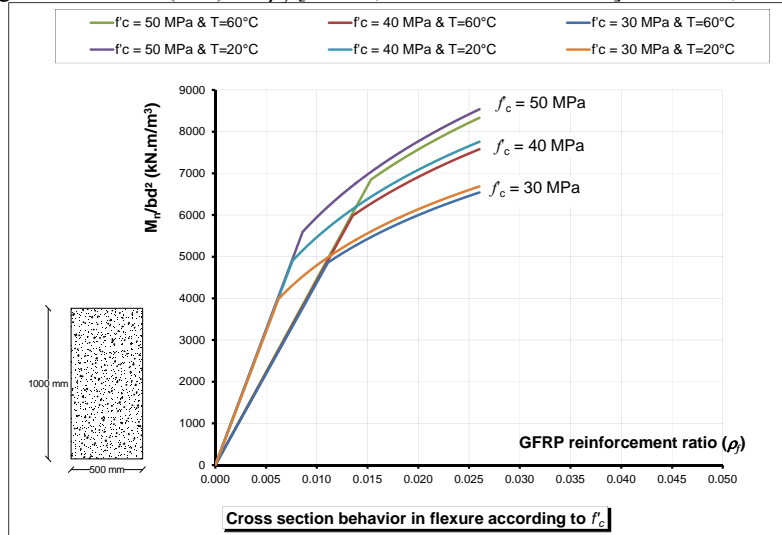Fig. 11 Live load (W_{LL}) vs. ρ_f [h=1 m, b=0.5 m and L=10 m] at 60°C d_b=16 mm

Fig. 12 Mn/bd^2 vs. ρ_f for various f'_c (30, 40 and 50 MPa) at 20°C, 60°C

3.6 Effect of the concrete compressive strength along with mean-ambient temperature

Chart 12, explains the effect of the change of concrete compressive strength along with the change in temperature. It shows (M_n/bd^2 vs. ρ_f) for a GFRP reinforced beam. The concrete uniaxial compressive strength ($f'c$) ranged from 25 MPa to 45 MPa. Two temperatures were considered; 20°C and 60°C. However, from these figures, it can be seen that when $f'c$ is increasing, the value of ρ_{fb} increases. Nevertheless, this increase is associated with an increase in the beam ultimate flexural strength. Moreover, as the temperature increases, the value of ρ_{fb} decreases. Also, the

decrease in flexural capacity is insignificant when $\rho_f > \rho_{fb}$ as the temperature increases from 20℃ to 60℃, while it is major when $\rho_f < \rho_{fb}$.

4. Conclusions

Based on the results of this research project, the following conclusions can be drawn:

1. When the reinforcement ratio is smaller than the balanced ratio, a slight increase in the amount of reinforcement is associated with a large increase in the flexural capacity of the beam. However, the increase in flexural capacity is modest when the reinforcement ratio is larger than that at the balanced condition.

2. An increase in the reinforcement ratio over the balanced ratio is coupled with a significant decrease in the bar stress. Therefore, it is not recommended to use beams with reinforcement ratio larger than twice the ratio of the balanced condition because the larger the amount of bars, the less efficient they are.

3. For beams reinforced with GFRP rebars, the higher the temperature, the lower the nominal flexural capacity.

4. As the temperature increases from 20°C to 60°C, the decrease in flexural capacity is insignificant when $\rho_f > \rho_{fb}$, while it is significant when $\rho_f < \rho_{fb}$.

5. For beam with spans to depth ratios of 5.0 or less, crack width limits usually control the design, however, for longer span beams, deflection tends to control the design.

6. It is not practical to use large diameter bars with large spacing because it increases the crack width, thus limiting the beam capacity.

7. The larger the applied external load, the more likely that deflection will control the design of FRP reinforced concrete beams.

8. Since the effect of bar diameter on the cracking load is critical, it is recommended that more bars with small diameter rather than fewer large diameter bars be used.

9. For beam with spans to depth ratios of more than 12, FRP rebars are not recommended for use as concrete reinforcement.

10. Unlike steel reinforced concrete beams, as $f'c$ increases, the value of ρ_{fb} increases.

11. Concrete compressive strength has significant effect on the flexural capacity of FRP reinforced concrete beams, while its influence is not as significant for steel reinforced concrete beams.

12. When the reinforcement ratio is within the recommended range, $\rho_{fb} < \rho_f < 1.25\rho_{fb}$, a beam reinforced by FRP has a larger flexural capacity when compared to a steel reinforced beam. In that range, the flexural strength of a GFRP reinforced concrete beam (RCB) is approximately 1.5 times the strength of a steel RCB.

References

Aboutaha, R. (2004), "Guide for maintenance, and rehabilitation of concrete bridge components with FRP composites - research into practice*"*, Syracuse University, Syracuse, NY, U.S.A.

Aboutaha, R. (2006), *"Evaluation and certification of GFRP bars ComBAR tests with respect to the requirements of the ACI 440.3R-04 Report"*, Syracuse University, Syracuse, NY, U.S.A.

ACI 440.1R-06, (2006), "Guide for the design and construction of structural concrete reinforced with FRP bars", American Concrete Institute (ACI).

ACI 318-05 and ACI 318R-05, (2005), "Building code requirement for structural concrete and commentary", American Concrete Institute (ACI).

Adimi, R., Rahman, H., Benmokrane, B. and Kobayashi, K. (1998), "Effect of temperature and loading frequency on the fatigue life of a CFRP bar in concrete", *Proceedings of the Second International Conference on Composites in Infrastructure (ICCI-98)*, Tucson, Ariz., **2**, 203-210.

American Composites Manufacturers Association, (2004), "*ABC's of FRP*", 1010 N. Glebe Road, Suite 450 Arlington, VA 22201.

Ando, N., Matsukawa, H., Hattori, A. and Mashima, A. (1997), "Experimental studies on the long term tensile properties of FRP tendons", *Proceedings of the Third International Symposium on Non-Metallic (FRP) Reinforcement for Concrete Structures (FRPRCS-3)*, **2**, Japan Concrete Institute, Tokyo, Japan, 203-210.

Bischoff, P.H. (2005), "Reevaluation of deflection prediction for concrete beams reinforced with steel and fiber reinforced polymer bars", *J. Struct. Eng.*, **131**(5), 752-767.

Bischoff, P.H. (2007a), "Deflection calculations of FRP reinforced concrete beams based on modifications to the existing Branson equation", *J. Compos. Constr.*, **11**(1), 4-14.

Bischoff, P.H. (2007b), "Rational model for calculating deflection of reinforced concrete beams and slabs", *Can. J. Civil Eng.*, **34**(8), 992-1002.

Bischoff, P.H., Gross, S. and Ospina, C.E. (2009), "The story behind proposed changes to ACI 440 deflection requirements for FRP-reinforced concrete", American Concrete Institute, ACI Special Publication (264 SP), 53-76.

Bischoff, P.H. and Gross, S.P. (2011), "Equivalent moment of inertia based on integration of curvature", *J. Compos. Constr.*, **15**(3), 263-273.

Bischoff, P.H. and Gross, S.P. (2011), "Design approach for calculating deflection of FRP-reinforced concrete", *J. Compos. Constr.*, **15**(4), 490-590.

Bootle, J., Burzesi, F. and Fiorini, L. (2001), "Design guidelines", *ASM Handbook*, **21**, Composites, ASM International, Material Park, Ohio, 388-395.

Branson, D.E. (1977), *Deformation of concrete structures*, McGraw-Hill Book Co., New York, 546.

Brown, V. (1997), "Sustained load deflections in GFRP reinforced concrete beams", *Proceedings of the Third International Symposium on Non-Metallic (FRP) reinforcement for Concrete Structures (FRPRCS-3)*, **2**, Japan Concrete Institute, Tokyo, Japan, 495-502.

Chang, K.K. (2001), "Aramid fibers", *ASM Handbook*, **21**, Composites, ASM International, Material Park, Ohio, 41-45.

Ehsani, M.R. (1993), "Glass-fiber reinforcing bars", *Alternative Materials for the Reinforcement and Prestressing of Concrete*, J. L. Clarke, Blackie Academic & Professional, London, 35-54.

Freimanis, A.J., Bakis, C.E., Nanni, A. and Gremel, D. (1998), "A comparison of pullout and tensile behaviors of FRP reinforcement for concrete", *Proceedings of the Second International Conference on Composites in Infrastructure (ICCI-98)*, **2**, Tucson, Ariz., 52-65.

Gao, D., Benmokrane, B. and Masmoudi, R. (1998a), "A calculating method of flexural properties of FRP-reinforced concrete beam: Part 1: Crack width and deflection", *Technical Report*, Department of Civil Engineering, University of Sherbrooke, Sherbrooke, Québec, Canada, 24.

Jaeger, L.G., Mufti, A. and Tadros, G. (1997), "The concept of the overall performance factor in rectangular-section reinforced concrete beams", *Proceedings of the Third International Symposium on Non-Metallic (FRP) Reinforcement for Concrete Structures (FRPRCS-3)*, **2**, Japan Concrete Institute, Tokyo, Japan, 551-558.

Kocaoz, S., Samaranayake, V.A. and Nanni, A. (2005), "Tensile characterization of glass FRP bars", *Compos. Part B*, **36**(1), 127-134.

Mallick, P.K. (1988), *Fiber reinforced composites, materials, manufacturing, and design*, Marcell Dekker, Inc., New York, 469.

Mutsuyoshi, H., Uehara, K. and Machida, A. (1990), "Mechanical properties and design method of concrete beams reinforced with carbon fiber reinforced plastics", *Transaction of the Japan Concrete Institute*, **12**, Japan Concrete Institute, Tokyo, Japan, 231-238.

Nucciarelli, B. (2007), "The controlling flexural limit states for GFRP reinforced concrete beams designed according to the ACI 440.1R-06 recommendations", Syracuse University, NY, USA.

Ospina, C.E. and Nannii, A. (2007), "Current FRP-reinforced concrete design trends in ACI 440.1R", University of Patras, Patras, Greece.

Ospina, C.E., Alexander, S. and Cheng, J.J. (2001), "Behavior of concrete slabs with fibre-reinforced polymer reinforcement", Structural Engineering Report No. 242, Department of Civil and Environmental Engineering, University of Alberta, 355.

Ospina, C.E. and Gross, S.P. (2005), "Rationale for the ACI 440.1R-06 indirect deflection control design provisions", *Proceedings, 7th Intl. Symposium on FRP Reinforcement for Concrete Structures*, Kansas City, USA, 651-670.

Shield, C.K., Galambos, T.V. and Gulbrandsen, P. (2011), "On the history and reliability of the flexural strength of FRP reinforced concrete members in ACI 440.1R", 10th International Symposium on Fiber Reinforced Polymer Reinforcement for Concrete Structures (FRPRCS-10), Tampa, Florida, USA.

Theriault, M. and Benmokrane, B. (1998), "Effects of FRP reinforcement ratio and concrete strength on flexural behavior of concrete beams", *J. Compos. Constr.*, **2**(1), 7-16.

Veysey, S. and Bischoff, P.H. (2011), "Designing FRP reinforced concrete for deflection control", 10th International Symposium on Fiber Reinforced Polymer Reinforcement for Concrete Structures (FRPRCS-10), Tampa, Florida, USA.

Wallenberger, F.T., Watson, J.C. and Hong, L. (2001), "Glass fibers", ASM Handbook, **21**, Composites, *ASM International*, Material Park, Ohio, 27-34.

Walsh, P.J. (2001), "Carbon fibers", *ASM Handbook*, **21**, Composites, ASM International, Material Park, Ohio, 35-40.

Wu, W.P. (1990), "Thermomechanical properties of fiber reinforced plastic (FRP) bars", PhD dissertation, West Virginia University, Morgantown, W.Va., 292.

Zheng, Y., Li, C. and Yu, G. (2012), "Behavior of laterally restrained GFRP reinforced concrete slab", The Third Asia-Pacific Conference on FRP in Structures (APFIS 2012), Hokkaido University, Japan.

CM

Notations

ACI	=	American Concrete Institute
A_f	=	Area of FRP bar, mm²
C_E	=	Environmental reduction factor
C	=	Distance from extreme compression fiber to the neutral axis, mm
$CFRP$	=	Carbon Fiber Reinforced polymer
CTE	=	Coefficient of Thermal Expansion, 1/C°
D	=	Distance from extreme compression fiber to centroid of tension reinforcement, mm
d_b	=	Diameter of reinforcing bar, mm
d_c	=	Thickness of concrete cover measured from extreme tension fiber to center of bar or wire location closest thereto, mm
E_c	=	Modulus of elasticity of concrete, MPa
E_f	=	Design or guaranteed modulus of sample of test specimens, MPa
f'_c	=	Specified compressive strength of concrete, MPa
f_f	=	Stress in FRP reinforcement in tension, MPa
f_{fu}	=	Design tensile strength of GFRP, considering reductions for service environment, MPa
f_{fu}^*	=	Guaranteed tensile strength of FRP bar, defined as mean tensile strength of sample of test specimens minus three times standard deviation, MPa
FRP	=	Fiber Reinforced Polymer
$GFRP$	=	Glass Fiber Reinforced polymer
I	=	Moment of inertia, mm^4
I_{cr}	=	Moment of inertia of transformed cracked section, mm^4
I_e	=	Effective moment of inertia, mm^4
I_g	=	Gross moment of inertia, mm^4
k	=	Ratio of depth of neutral axis to reinforcement depth
M_a	=	Maximum moment in member at stage deflection is computed, KN.m
M_{cr}	=	Cracking moment, KN.m
M_n	=	Nominal moment capacity, KN.m
M_s	=	Moment due to sustained load, KN.m
M_u	=	Factored moment at section, KN.m
n_f	=	Ratio of modulus of elasticity of FRP bars to modulus of elasticity of concrete
s	=	longitudinal FRP bar spacing, mm
w	=	Maximum crack width, mm
α_L	=	Longitudinal coefficient of thermal expansion, 1/C°
β	=	Ratio of distance from neutral axis to extreme tension fiber to distance from neutral axis to center of tensile reinforcement
β_1	=	Factor taken as 0.85 for concrete f'_c up to and including 28 MPa. For strength above 28 MPa, this factor is reduced continuously at a rate of 0.05 per each 7 MPa of strength in excess of 28 MPa, but is not taken less than 0.65
β_d	=	Reduction coefficient used in calculating deflection
$\Delta_{(cp+sh)}$	=	Additional deflection due to creep and shrinkage under sustained loads, mm
$(\Delta_i)_{sus}$	=	Immediate deflection due to sustained loads, mm

ε_c	=	Strain in concrete
ε_{cu}	=	Ultimate strain in concrete
ε_f	=	Strain in FRP reinforcement
ε_{fu}	=	Strain in FRP reinforcement
ε_{fu}^*	=	Guaranteed rupture strain of FRP reinforcement, defined as the mean tensile strain of sample of test specimens minus three times standard deviation, mm/mm
$\varepsilon_{u,ave}$	=	mean tensile strain of sample of test specimens,
λ	=	Multiplier for additional long term deflection
ξ	=	Time dependent factor for sustained load
ρ_f	=	FRP reinforcement ratio
ρ_f'	=	Ratio of FRP compression reinforcement
ρ_{fb}	=	FRP reinforcement ratio producing balanced strain conditions
ϕ	=	Strength reduction factor